Original Research Paper

In-silico FDA-approved drug repurposing to find the possible treatment of Coronavirus Disease-19 (COVID-19)

Kumar Sharp[1], Dr. Shubhangi Dange[2]*

[1]2nd MBBS undergraduate student, Government Medical College and Hospital, Jalgaon

[2]Associate Professor, Dept. of Microbiology, Government Medical College and Hospital, Jalgaon

*Corresponding author: -
Dr. Shubhangi Dange,
Associate Professor,
Department of Microbiology,
Government Medical College and Hospital, Jalgaon
Email: dangeshubhangi@gmail.com

Abstract

Identification of potential drug-target interaction for approved drugs serves as the basis of repurposing drugs. Studies have shown polypharmacology as common phenomenon. In-silico approaches help in screening large compound libraries at once which could take years in a laboratory. We screened a library of 1050 FDA-approved drugs against spike glycoprotein of SARS-CoV2 in-silico. Anti-cancer drugs have shown good binding affinity which is much better than hydroxychloroquine and arbidol. We have also introduced a hypothesis named "Bump" hypothesis which and be developed further in field of computational biology.

Keywords: spike glycoprotein; FDA; drug repurposing; anti-cancer; hydroxychloroquine

Introduction

Identification of potential drug-target interaction for approved drugs serves as the basis of repurposing drugs. Studies have shown polypharmacology as common phenomenon [1][2]. Since the three-dimensional structures of proteins of SARS-CoV2 have been mapped it opens opportunity for in-silico approaches of either novel drug discovery or drug repurposing. In the absence of an exact cure or vaccine, coronavirus disease-19 has taken a huge toll of humanity. Our study of target specific drug docking and novel hypothesis contributes in this fight. In-silico approaches help in screening large compound libraries at once which could take years in a laboratory. This accelerates the process of drug discovery which can then be specifically to laboratory studies and thus save time, cost and resources which are crucial in such situation of a pandemic.

Methodology:

The three-dimensional structure of receptor-binding domain (RBD) of spike glycoprotein of SARS-CoV2 and angiotensin-converting enzyme ACE 2 receptor complex 6M0J was obtained from Protein Data Bank [3] (Figure 1). Chain A is ACE 2 receptor and chain E is RBD. The active sites were derived from the article by Lan et al [4]. As mentioned, 15 target amino acid sites of chain E which help in binding with chain A would be our target amino acids.
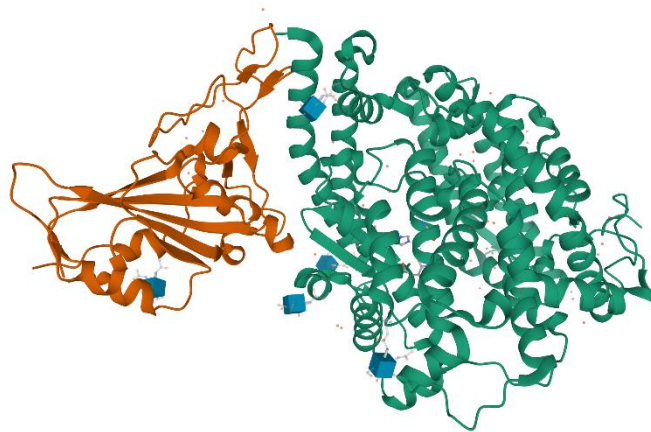

Figure 1: Three-dimensional structure of spike glycoprotein RBD chain E and ACE2 receptor chain A complex 6M0J. Chain E is coloured orange and chain A is coloured green.

These 15 amino acid targets along with their position in the sequence is as follows:

1. Tyr449
2. Tyr453
3. Asn487
4. Tyr489
5. Gly496
6. Thr500
7. Gly502
8. Tyr505
9. Leu455
10. Phe456
11. Phe486
12. Gln493
13. Asn501
14. Gln498
15. Lys417

The above standard abbreviations are: Tyr: Tyrosine; Asn: Asparagine; Gly: Glycine; Thr: Threonine; Leu: Leucine; Phe: Phenylalanine; Gln: Glutamine; Lys: Lysine.

The last amino acid Lys417 helps in salt-bridge formation between chain E and A and is believed to be the reason for strong binding affinity as this was absent in SARS-CoV. Leu455, Phe486, Gln493 and Asn501 are the amino acids in SARS-CoV2 whose corresponding amino acids in SARS-CoV were important in binding. The above 5 amino acids will be our preferences when selecting results among docked drugs.

1050 FDA-approved drug structures were obtained from Zinc15 database [5]. Arbidol and hydroxychloroquine structures were also taken separately for analysis because of their role to prevent virus entry into the cell [6]. The docking software used in this study is PyRx virtual screening tool because of its user-friendly graphical user-interface and inclusion of Autodock Vina and Open Babel within its environment [7][8][9]. These programs are necessary for preparation of ligand and receptor before docking and the docking itself.

After obtaining the necessary conditions like three-dimensional structure of receptor, ligand structure database and target amino acids, docking was proceeded with PyRx. The receptor complex 6M0J was loaded and only chain E was extracted from the structure. The chain E was converted to Autodock macromolecule by automatic removal of water molecules, addition of hydrogen atoms and addition of partial charges. The drug structures were loaded in PyRx Open Babel plug-in. All drug structures were minimized to have the least conformational energy. The minimized structures were then converted into Autodock ligands by automatic addition of hydrogen atoms and addition of partial charges to the system.

The Vina search space was set in PyRx so as to included all 15 target amino acids (figure 2). The co-ordinate data of the search space is as follows:

center_x = -36.6861

center_y = 28.5454

center_z = 3.8350

size_x = 19.2344

size_y = 39.4447

size_z = 21.2095

The docking was proceeded with maximum exhaustiveness of 8 modes. The study was conducted on a Windows 10 64-bit operating system. The entire docking took about 11 hours with 100% CPU utilization.
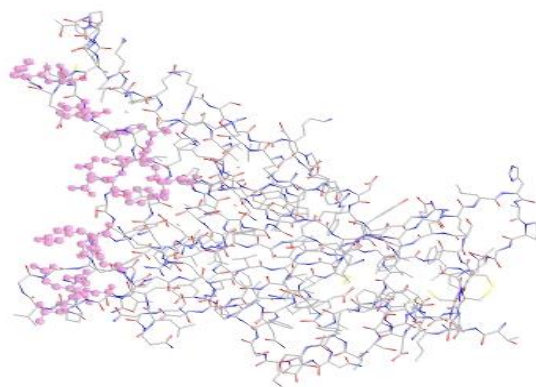
Figure 2: Chain E in line representation with target amino acid position highlighted in pink.

The results obtained were then sorted in increasing order of binding energy in kcal/mol (kilocalorie per mole) since lower the binding affinity value stronger is the binding between ligand and receptor. Only modes with zero root mean square deviation were considered to obtain the best docking possible. The results were evaluated till a binding affinity of -7.5 kcal/mol.
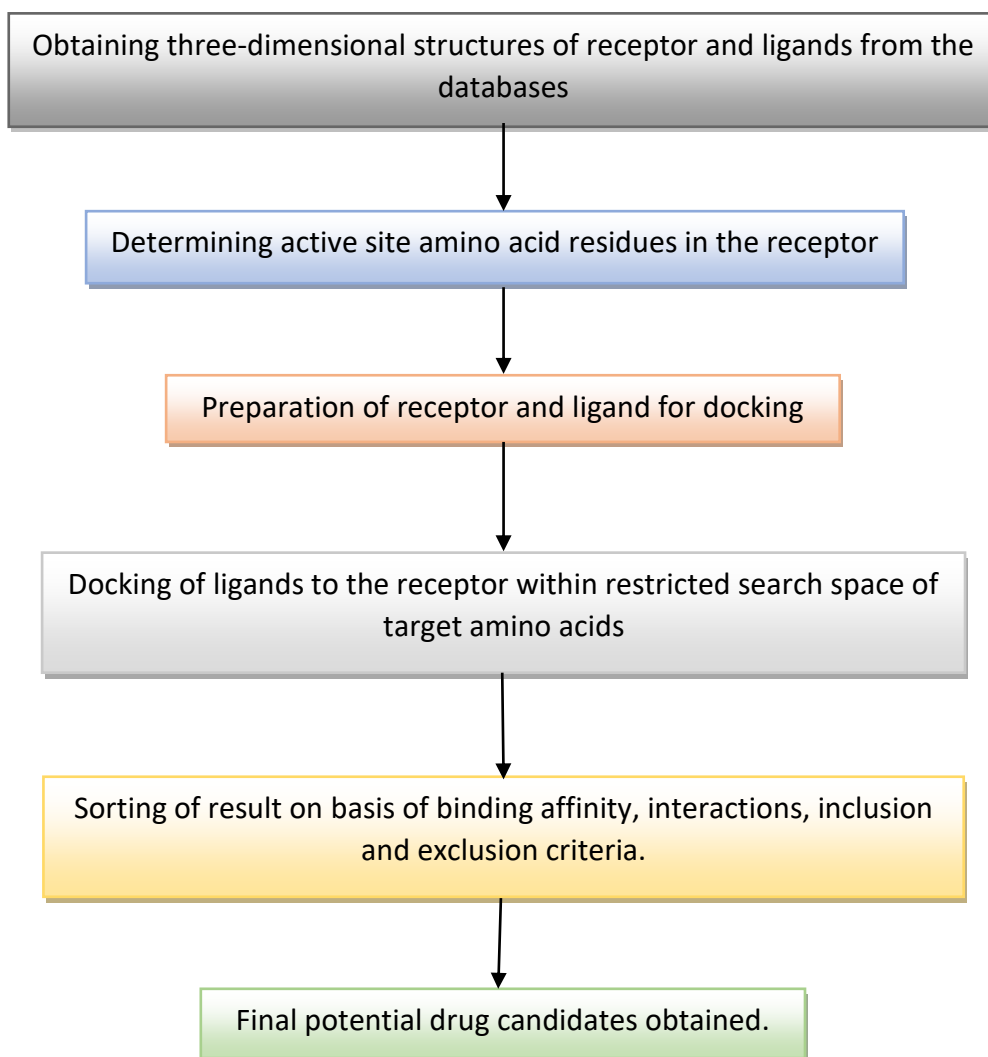
All ligand-receptor interactions were visualized using Drug Discovery Studio [10]. The two-dimensional diagrams of all the result ligand interactions with the receptor were obtained. The receptor refers to chain E or the receptor-binding domain of the spike glycoprotein. The amino acid with which interactions occur were noted.

Filter of results to choose the best drug candidate was done on basis of two inclusion criteria:

1. How many of the desired target amino acids did that drug interact with?
2. How many of the preferred 5 target amino acids did that drug interact with?

Any drug interaction which was determined to be unfavourable was removed from the study and hence constituted the exclusion criteria. According to the above two conditions, the result drugs were sorted in decreasing order of number of interactions. A final list of potential drug candidates was prepared according to the above two filter results. These drug candidates were then visualized in Drug Discovery Studio to show unfavourable binding to chain A i.e. ACE2 receptor and thus proving the effectiveness of the drug when it is bond to RBD.

The above methodology is summarized as follows:

Obtaining three-dimensional structures of receptor and ligands from the databases

↓

Determining active site amino acid residues in the receptor

↓

Preparation of receptor and ligand for docking

↓

Docking of ligands to the receptor within restricted search space of target amino acids

↓

Sorting of result on basis of binding affinity, interactions, inclusion and exclusion criteria.

↓

Final potential drug candidates obtained.

Results:

Molecular docking between FDA-approved drug ligands and chain E of 6M0J was completed and results were sorted in increasing order of binding energy till -7.5kcal/mol. Only RMSD value of zero results were considered as they indicated the best binding conformation as compared to other modes. The results obtained are in the table below (Table 1):

Ligand receptor complex	Binding Affinity (kcal/mol)	Name (as per Zinc15 database)
6m0j_E_ZINC000027990463_uff_E=654.95	-8.2	lomitapide
6m0j_E_ZINC000052955754_uff_E=965.09	-8.2	ergotamine
6m0j_E_ZINC000006716957_uff_E=651.98	-8.2	nilotinib
6m0j_E_ZINC000003978005_uff_E=940.58	-8.1	dihydroergotamine
6m0j_E_ZINC000029416466_uff_E=554.86	-8	saquinavir
6m0j_E_ZINC000066166864_uff_E=877.49	-8	alectinib
6m0j_E_ZINC000026664090_uff_E=535.51	-7.9	saquinavir
6m0j_E_ZINC000036701290_uff_E=764.28	-7.8	ponatinib
6m0j_E_ZINC000068153186_uff_E=1005.56	-7.8	dabrafenib
6m0j_E_ZINC000068204830_uff_E=1113.83	-7.7	daclatasvir
6m0j_E_ZINC000003817234_uff_E=983.51	-7.7	celsentri
6m0j_E_ZINC000019632618_uff_E=489.47	-7.7	imatinib
6m0j_E_ZINC000049036447_uff_E=1212.85	-7.6	suvorexant
6m0j_E_ZINC000000896717_uff_E=1163.37	-7.6	accolate
6m0j_E_ZINC000012503187_uff_E=1067.62	-7.6	conivaptan
6m0j_E_ZINC000035328014_uff_E=725.43	-7.5	ibrutinib
6m0j_E_ZINC000084668739_uff_E=1140.66	-7.5	lifitegrast
6m0j_E_ZINC000095551509_uff_E=4776.36	-7.5	grazoprevir
6m0j_E_ZINC000000538312_uff_E=544.51	-7.5	risperdal
6m0j_E_ZINC000001542113_uff_E=741.62	-7.5	vilazodone
6m0j_E_ZINC000001996117_uff_E=701.60	-7.5	darifenacin
6m0j_E_ZINC000003816287_uff_E=509.48	-7.5	axitinib
6m0j_E_ZINC000003881958_uff_E=3.2e+265	-7.5	danol
6m0j_E_ZINC000011681534_uff_E=315.75	-7.5	nebivolol
---	---------------------	--------------------
Arbidol 19907652	-6	arbidol
HCQ 1530652	-5.7	hydroxychloroquine

Table 1: Results of docking as per binding affinity till -7.5 kcal/mol.

The ligand interactions of all the above structures were analysed in Drug Discovery Studio and the following results was obtained as given in Table 2. The interactions of ligands are mentioned with standard amino acid abbreviations and if any unfavourable interactions the ligand is marked in red and its interactions are not considered.

Ligand receptor complex	Binding Affinity	Interactions	Name
6m0j_E_ZINC000027990463_uff_E=654.95	-8.2	1. UNFAVOURABLE	lomitapide
6m0j_E_ZINC000052955754_uff_E=965.09	-8.2	2. tyr505; gly496; arg403	ergotamine
6m0j_E_ZINC000006716957_uff_E=651.98	-8.2	3. thr500; tyr449; tyr453; ser494; tyr495; gln493; arg403; gly496	nilotinib
6m0j_E_ZINC000003978005_uff_E=940.58	-8.1	4. UNFAVOURABLE	dihydroergotamine
6m0j_E_ZINC000029416466_uff_E=554.86	-8	5. UNFAVOURABLE	saquinavir
6m0j_E_ZINC000066166864_uff_E=877.49	-8	6. tyr505; arg403; tyr453; lys417	alectinib
6m0j_E_ZINC000026664090_uff_E=535.51	-7.9	7. gly496; tyr505; tyr453; gln493; arg403; leu455	saquinavir
6m0j_E_ZINC000036701290_uff_E=764.28	-7.8	8. leu455; gln493; tyr495; tyr505; phe497; arg403; gly496; gln498; asn501	ponatinib
6m0j_E_ZINC000068153186_uff_E=1005.56	-7.8	9. lys417; tyr453; tyr449; gln493; tyr505; gly496; asn501	dabrafenib
6m0j_E_ZINC000068204830_uff_E=1113.83	-7.7	10.tyr489; phe456; leu455; tyr453; tyr495; arg403; gly496	daclatasvir
6m0j_E_ZINC000003817234_uff_E=983.51	-7.7	11.gln493; leu455; tyr453; glu406; lys417	celsentri
6m0j_E_ZINC000019632618_uff_E=489.47	-7.7	12.thr500; gln493; gly496; tyr505; glu484	imatinib
6m0j_E_ZINC000049036447_uff_E=1212.85	-7.6	13.tyr505; arg403; tyr453; lys417; ser494	suvorexant
6m0j_E_ZINC000000896717_uff_E=1163.37	-7.6	14.gln493; tyr453; tyr449; lys417; tyr505; phe497; arg403; tyr495	accolate
6m0j_E_ZINC000012503187_uff_E=1067.62	-7.6	15.lys417; leu455; tyr449; tyr453	conivaptan
6m0j_E_ZINC000035328014_uff_E=725.43	-7.5	16.arg403; tyr453; lys417; tyr449; ser494	ibrutinib
6m0j_E_ZINC000084668739_uff_E=1140.66	-7.5	17.gly496; ser494; gln493; phe456; tyr489; leu455	lifitegrast
6m0j_E_ZINC000095551509_uff_E=4776.36	-7.5	18.tyr453; gln493; ser494; tyr505; arg403; tyr449; leu455	grazoprevir
6m0j_E_ZINC000000538312_uff_E=544.51	-7.5	19.gly496; tyr505	risperdal
6m0j_E_ZINC000001542113_uff_E=741.62	-7.5	20.gly496; leu455; tyr505; gln493; glu484; phe490	vilazodone

6m0j_E_ZINC000001996 117_uff_E=701.60	-7.5	21.gln493; tyr505; gln498; ser494; gly496	darifenacin
6m0j_E_ZINC000003816 287_uff_E=509.48	-7.5	22.UNFAVOURABLE	axitinib
6m0j_E_ZINC000003881 958_uff_E=3.2e+265	-7.5	23.tyr505; arg403; tyr453	danol
6m0j_E_ZINC000011681 534_uff_E=315.75	-7.5	24.tyr453; arg403; gly496; tyr449; gln498; asn501; tyr505	nebivolol
------------------------------	------------	--	
Arbidol 19907652	-6	25.tyr453; tyr449; tyr505	arbidol
HCQ 1530652	-5.7	26.UNFAVOURABLE	hydroxychl oroquine

Table 2: Ligand interactions as visualized in Drug Discovery Studio. Any ligand showing unfavourable interaction is marked in red.

The interaction results now obtained are filtered on the basis of number of desired target amino acids. Ligands also interact with other amino acids in the search space hence the count is on the basis of the 15 target amino acids as mentioned earlier. The top 10 drugs are as follows:

1. Dabrafenib-7/15
2. Ponatinib-6/15
3. Nebivolol-6/15
4. Nilotinib-5/15
5. Saquinavir-5/15
6. Daclatasvir-5/15
7. Accolate-5/15
8. Grazopevir-5/15
9. Celsentri-4/15
10. Imatinib-4/15

The interaction results were then filtered on the basis of the number of preferred 5 amino acid targets as mentioned above. The top 10 drugs are as follows:

1. Pontatinib-3/5
2. Dabrafenib-3/5
3. Celsentri-3/5
4. Saquinavir-2/5
5. Accolate-2/5
6. Conivaptan-2/5
7. Lifitegrast-2/5
8. Grazoprevir-2/5
9. Vilazodone-2/5
10. Nilotinib-1/5

The scores in the above two lists indicate: number of amino acid as per condition/total number of amino acids to be considered as per condition. They are arranged in decreasing order. In case they have the same results, they are sorted amongst themselves in order of binding affinity as per table 1 in increasing order.

On the basis of the above two lists the top 5 final drug candidates chosen are:

1. Dabrafenib (figure 3 and 9)
2. Ponatinib (figure 4 and 10)
3. Nilotinib (figure 5 and 11)
4. Saquinavir (figure 6 and 12)
5. Accolate (figure 7 and 13)

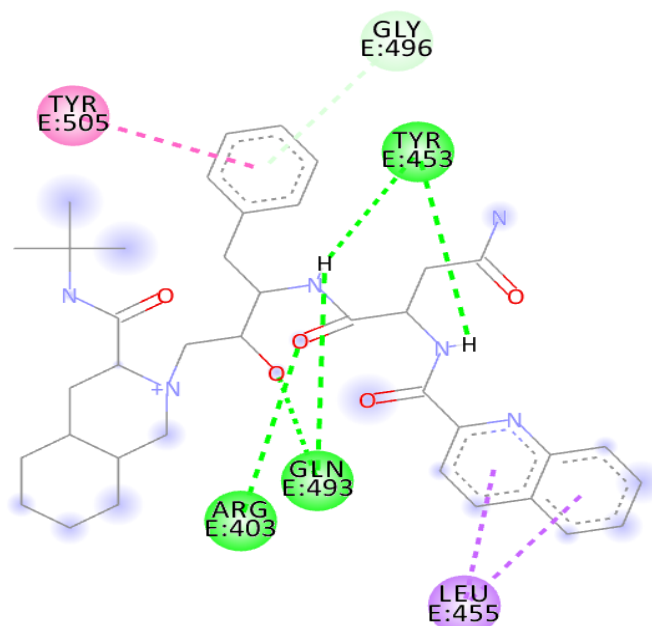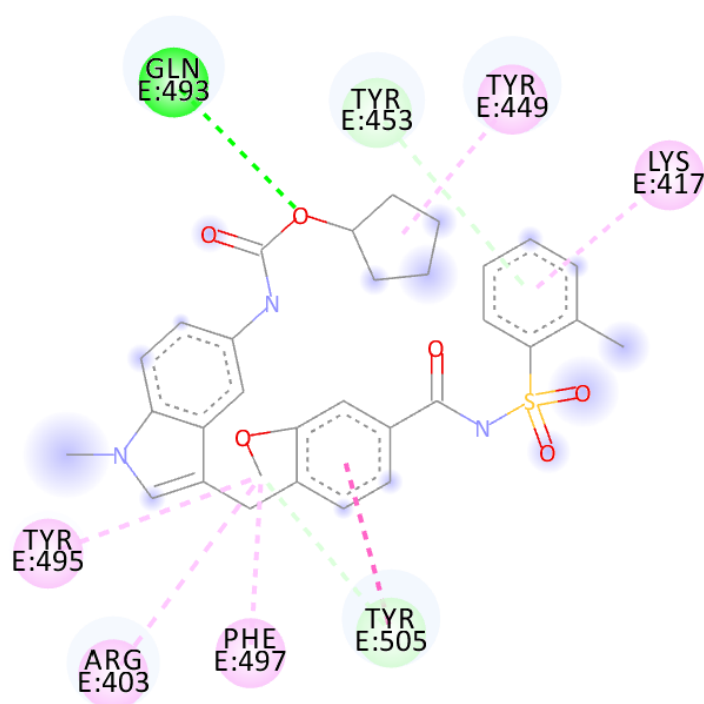Their structures and drug interactions are shown below:
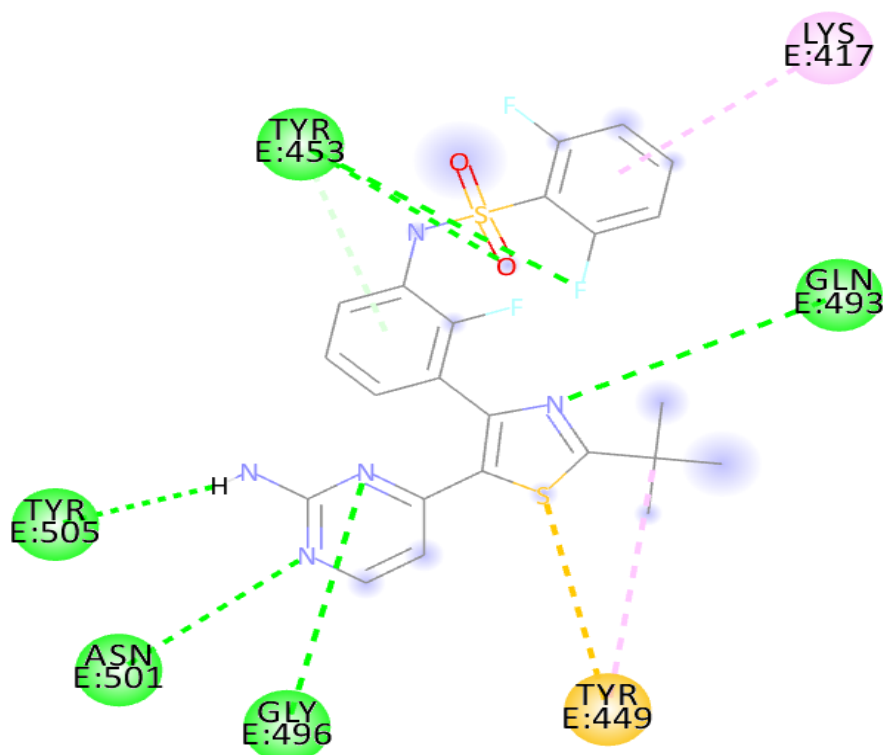
Figure 3: Dabrafenib (2D structure) in interaction with amino acids of chain E (circles with sequence position of that amino acid). Green bonds are the conventional hydrogen bonds. Pi-alkyl bonds are depicted in pink. Pi-sulphur bonds are depicted in yellow. Pi-donor hydrogen bond is depicted in light blue.
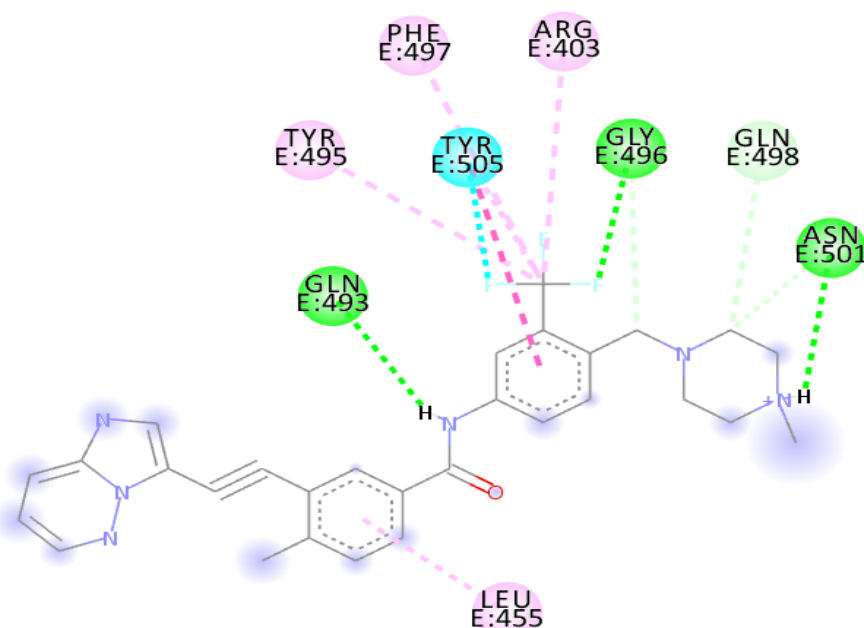
Figure 4: Ponatinib (2D structure) in interaction with amino acids of chain E (circles with sequence position of that amino acid). Green bonds are the conventional hydrogen bonds. Pi-alkyl and alkyl bonds are depicted in pink. Pi-Pi T shaped bonds are depicted in magenta. Halogen bond is depicted in blue. Carbon-Hydrogen bonds are depicted in light blue.
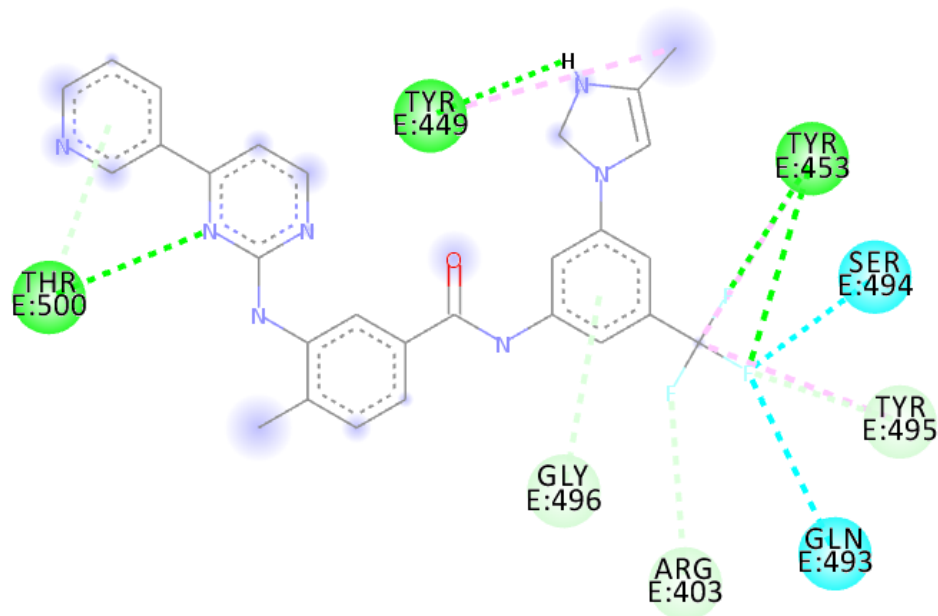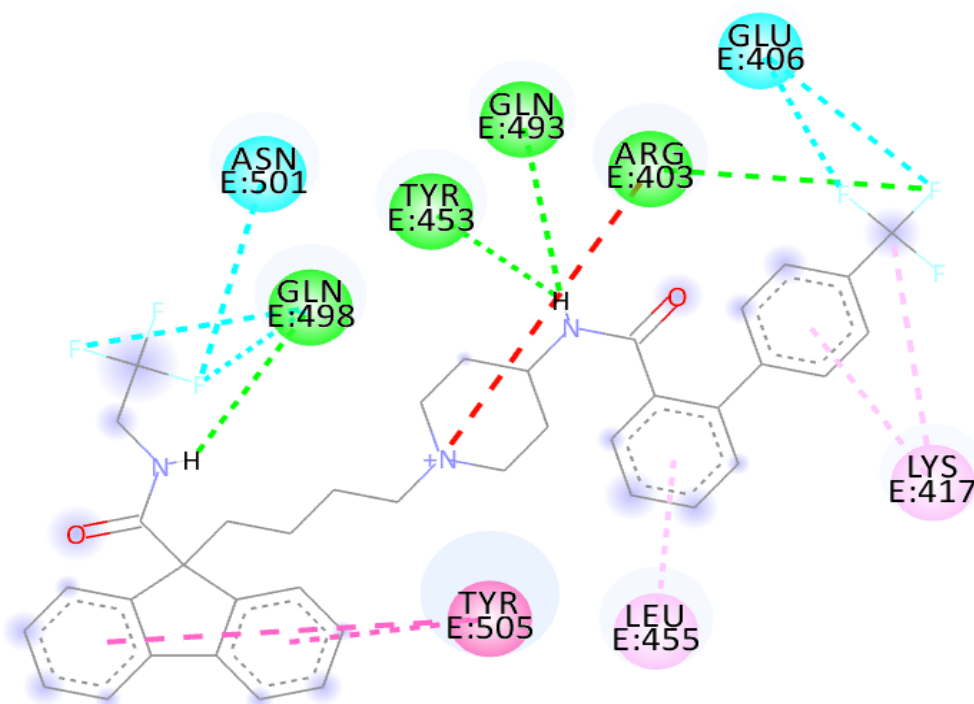

Figure 5: Nilotinib (2D structure) in interaction with amino acids of chain E (circles with sequence position of that amino acid). Green bonds are the conventional hydrogen bonds. Pi-alkyl bonds are depicted in pink. Halogen bond is depicted in blue. Carbon-Hydrogen and Pi-donor hydrogen bonds are depicted in light blue.

Figure 6: Saquinavir (2D structure) in interaction with amino acids of chain E (circles with sequence position of that amino acid). Green bonds are the conventional hydrogen bonds. Pi-Pi T shaped bonds are depicted in magenta. Pi-sigma bond is depicted in purple. Pi-donor hydrogen bonds are depicted in light blue.

Figure 7: Accolate (2D structure) in interaction with amino acids of chain E (circles with sequence position of that amino acid). Green bonds are the conventional hydrogen bonds. Pi-Pi T shaped and Pi-Pi stacked bonds are depicted in magenta. Pi-donor hydrogen and carbon hydrogen bonds are depicted in light blue. Alkyl and Pi-alkyl bonds are depicted in pink.

An interaction figure of lomitapide (from table 2) is also show as an example of unfavourable interaction below (figure 8 and 14):

Figure 8: Lomitapide (2D structure) in interaction with amino acids of chain E (circles with sequence position of that amino acid). Green bonds are the conventional hydrogen bonds. Pi-Pi stacked bonds are depicted in magenta. Halogen bonds are depicted in blue. Alkyl and Pi-alkyl bonds are depicted in pink. Unfavourable positive-positive bond is depicted in red.

The 2-dimensional structure of the drugs from Zinc15 database is shown below:
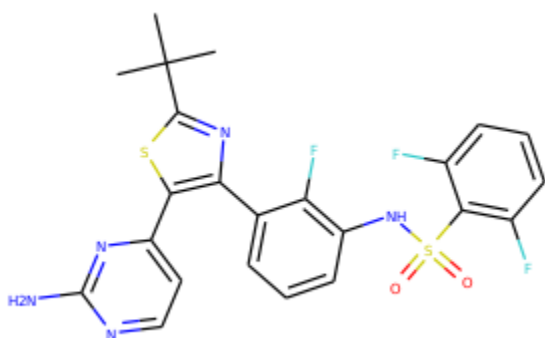
Figure 9: Dabrafenib   Figure 10: Ponatinib
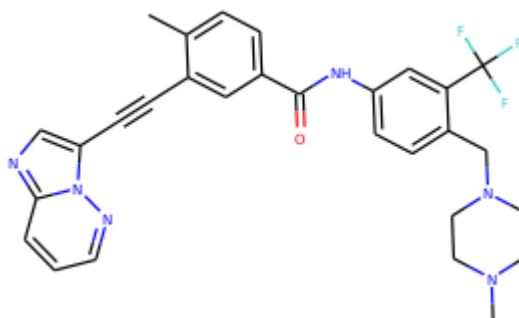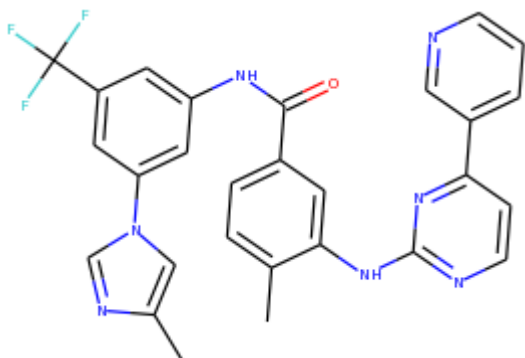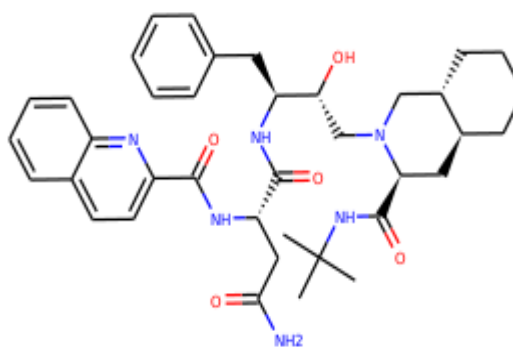
Figure 11: Nilotinib

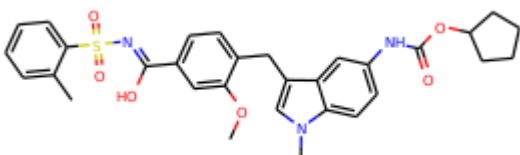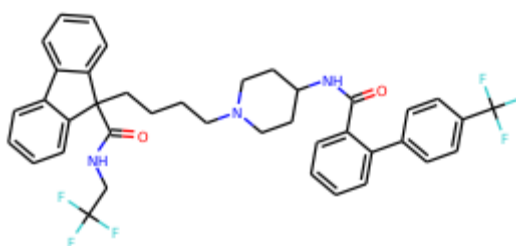

Figure 12: Saquinavir

Figure 13: Accolate

Figure 14: Lomitapide

Discussion

With the results obtained above, we find that hydroxychloroquine which is the prevalent treatment for novel coronavirus 2019 has the lowest affinity of -5.7 kcal/mol as well as unfavourable interactions. Arbidol which also is used to prevent viral entry has less binding affinity that other compounds which we found. Dabrafenib is approved for cancer with BRAF gene mutation. It has shown MERS-CoV: 45% inhibition at 10 micromolar concentration [11]. Ponatinib is used for treatment of chronic myelogenous leukemia, acute lymphocytic leukemia. It is a tyrosine kinase inhibitor and has also been shown to act on 2019-nCoV main protease [12]. Thus, this drug can affect dual targets of spike glycoprotein and main protease of the coronavirus. Nilotinib which is also used for treatment of chronic myelogenous leukemia has shown to inhibit MERS-CoV at 5.5 micromolar and SARS-CoV at 2.1 micromolar concentration [13]. Saquinavir is a drug used in anti-retroviral therapy has been shown to produce anti-viral activity against SARS-CoV2 in a study conducted in Shanghai [14]. Accolate is the tradename for zafirlukast which is a leukotriene receptor antagonist which is one among the drugs in a United Sates patent of human rhinovirus antibodies as a second therapeutic agent or antibody [15]. The results we have obtained above must be proceeded for in-vitro and in-vivo screening due to limitations of in-silico screening. The ligand and protein models used for in-silico study are strictly rigid unlike when present in biological systems. Multi-drug combination studies cannot be done in-silico [16]. Yet, the results we have obtained are very encouraging to proceed with. While analysing the results we also formed a hypothesis. The hypothesis is: "A drug attaches itself to the spike glycoprotein(ligand) and forms favourable bond with it. When this drug-ligand complex approaches the receptor, unfavourable bumps between the drug and receptor prevents binding of ligand and creates

repulsion. This prevents the binding of ligand and receptor and thus prevents the entry of the virus inside the cell." We named this hypothesis as the "Bump" hypothesis. A word of caution to prevent confusion, the drugs we consider for this hypothesis don't form unfavourable bonds with spike glycoprotein, example lomitapide in figure 8. The drugs like dabrafenib, ponatinib, nilotinib, saquinavir and accolate from favourable bonds with spike glycoprotein and unfavourable bonds in that position with ACE2 receptor. One such example is shown below in figure 15.
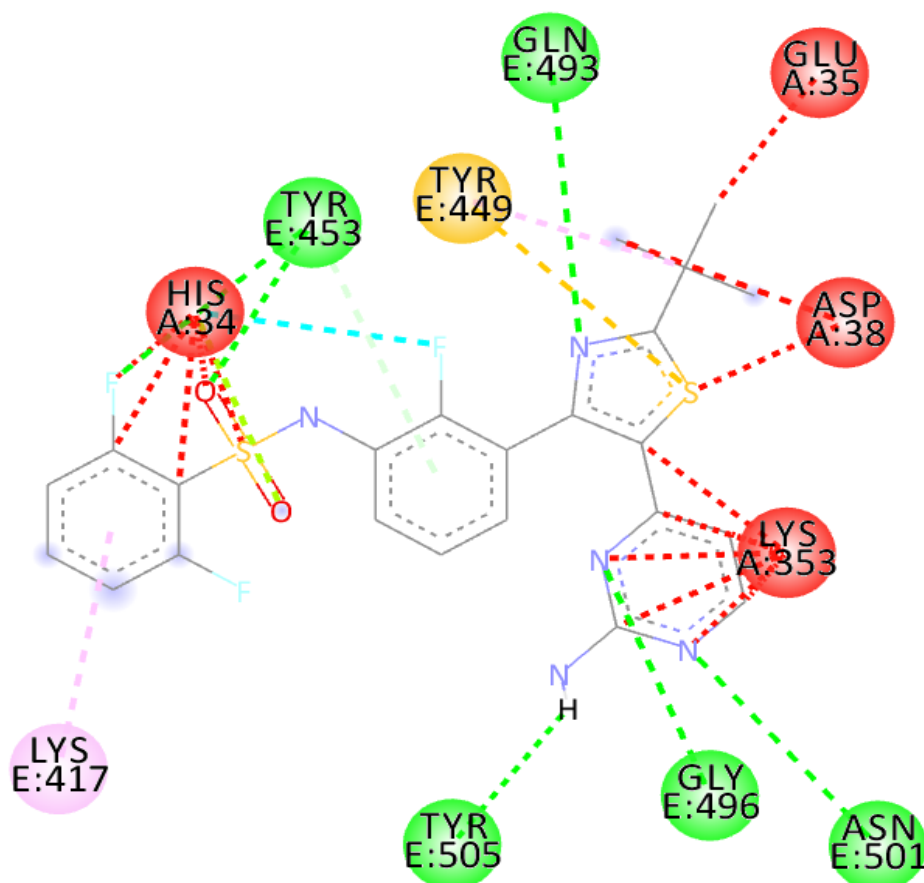

Figure 15: Dabrafenib (2D structure) in interaction with amino acids of chain E (circles with sequence position of that amino acid) and chain A (circles with sequence position of that amino acid). Green bonds are the conventional hydrogen bonds. Pi-alkyl bonds are depicted in pink. Pi-sulphur bonds are depicted in yellow. Pi-donor hydrogen bond is depicted in light blue. Unfavourable bonds are depicted in red with the interacting amino acid sequence.

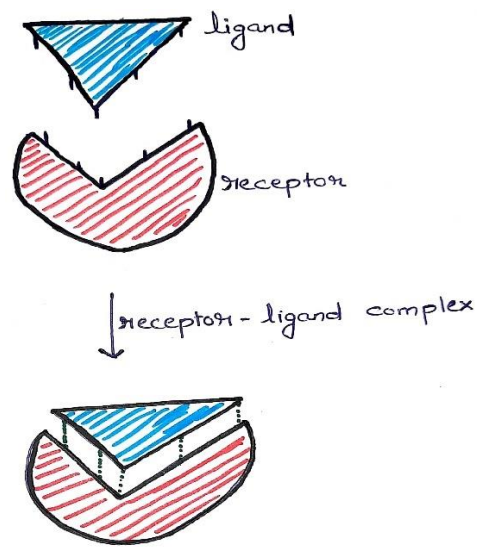We have illustrated our hypothesis in the below drawings:

Figure 16: A typical ligand-receptor interaction in absence of drugs. Active sites are indicated by projections from surfaces of both ligand and receptor.
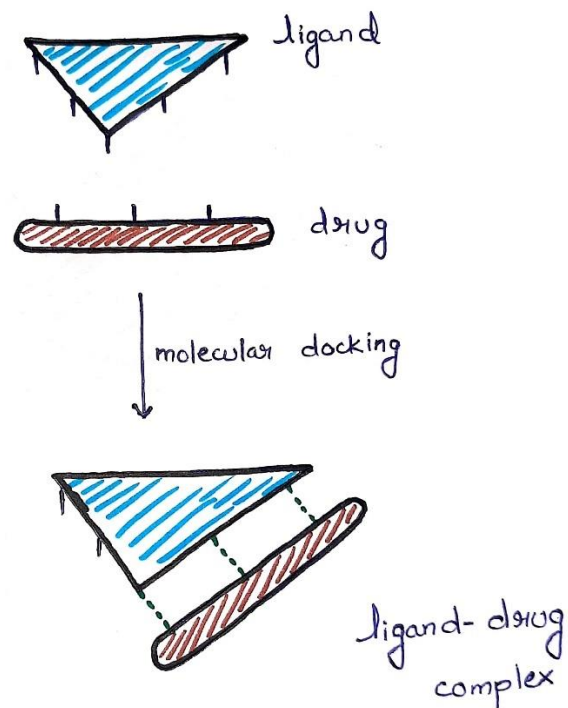

Figure 17: A drug interacts with the ligand and cover its active sites forming favourable interactions between them. This ligand-drug complex then approaches the receptor.
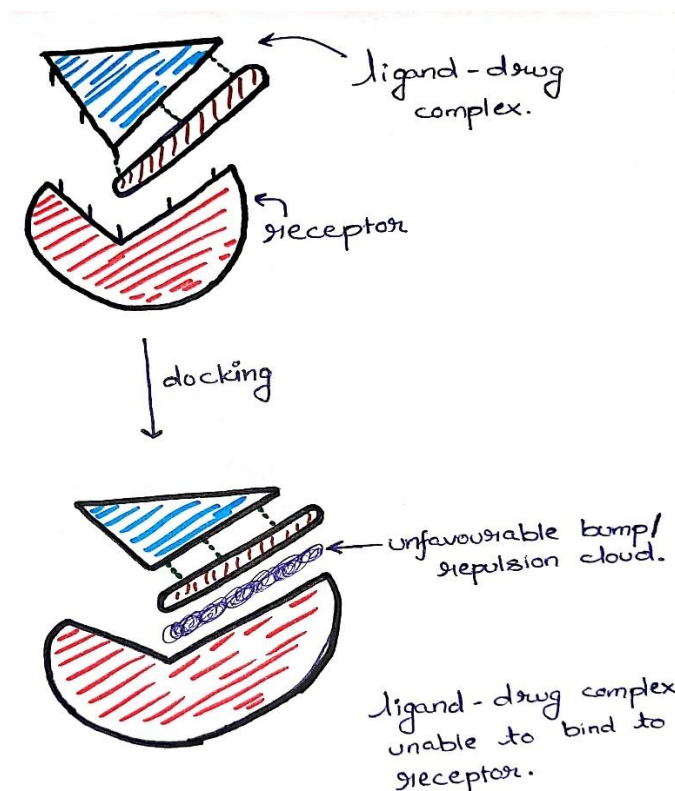
Figure 18: The ligand-drug complex approaches the target receptor for interaction. The drug has however covered most of the active sites of the ligand and the presence of drug is producing unfavourable bumps or repulsion cloud from the receptor. This overall minimizes the interaction and further action example viral entry fails.
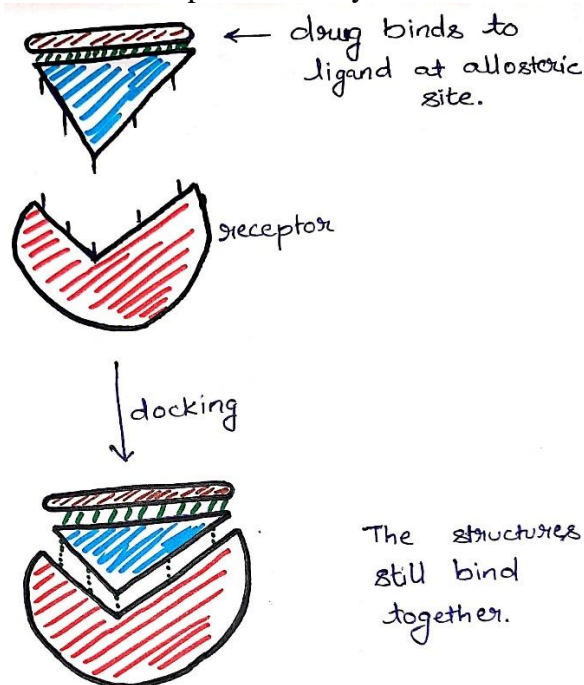

Figure 19: This illustration depicts a drug which binds to an allosteric site of ligand, yet the docking of ligand and receptor occurred failing its very purpose. This is one of the limitations of in-silico drug screening where models are strictly rigid and don't change their conformation unlike the case of allosteric/non-competitive inhibition in biological systems. Our above hypothesis requires further work to improve but the drugs we propose by in-silico screening must definitely be forwarded for in laboratory analysis.

Conclusion

In this study we have screened a large library of FDA-approved drugs and put forth promising results. We have highlighted the efficiency as well as limitations of in-silico screening. A critical hypothesis is also proposed which might stir further interest of computational biology. At times of this ongoing pandemic, our study might contribute in the fight against coronavirus. Our results though encouraging, must be tested in laboratory before proceeding with human trials and public use.

Source of funding: Nil

Ethical approval: Not required

Conflict of interest: The authors hereby declare no conflict of interests.

Contribution: All authors have equally contributed in the study.

References:

1. Law V, Knox C, Djoumbou Y, Jewison T, Guo AC, Liu Y, Maciejewski A, Arndt D, Wilson M, Neveu V, Tang A. DrugBank 4.0: shedding new light on drug metabolism. Nucleic acids research. 2014 Jan 1;42(D1): D1091-7.
2. Wang J, Ge Y, Xie XQ. Development and testing of druglike screening libraries. Journal of chemical information and modeling. 2018 Dec 18;59(1):53-65.
3. Bank PD. Protein data bank. Nature New Biol. 1971; 233:223.
4. Lan J, Ge J, Yu J, Shan S, Zhou H, Fan S, Zhang Q, Shi X, Wang Q, Zhang L, Wang X. Structure of the SARS-CoV-2 spike receptor-binding domain bound to the ACE2 receptor. Nature. 2020 Mar 30:1-6.
5. Sterling T, Irwin JJ. ZINC 15–ligand discovery for everyone. Journal of chemical information and modelling. 2015 Nov 23;55(11):2324-37.
6. Sanders JM, Monogue ML, Jodlowski TZ, Cutrell JB. Pharmacologic treatments for coronavirus disease 2019 (COVID-19): a review. Jama. 2020 Apr 13.
7. Dallakyan S, Olson AJ. Small-molecule library screening by docking with PyRx. InChemical biology 2015 (pp. 243-250). Humana Press, New York, NY.
8. Trott O, Olson AJ. AutoDock Vina: improving the speed and accuracy of docking with a new scoring function, efficient optimization, and multithreading. Journal of computational chemistry. 2010 Jan 30;31(2):455-61.
9. O'Boyle NM, Banck M, James CA, Morley C, Vandermeersch T, Hutchison GR. Open Babel: An open chemical toolbox. Journal of cheminformatics. 2011 Dec;3(1):33.
10. Ref. Dassault Systèmes BIOVIA, Discovery Studio Modeling Environment, Release 2017, San Diego: Dassault Systèmes, 2016.
11. Kindrachuk J, Ork B, Hart BJ, Mazur S, Holbrook MR, Frieman MB, Traynor D, Johnson RF, Dyall J, Kuhn JH, Olinger GG. Antiviral potential of ERK/MAPK and PI3K/AKT/mTOR signaling modulation for Middle East respiratory syndrome coronavirus infection as identified by temporal kinome analysis. Antimicrobial agents and chemotherapy. 2015 Feb 1;59(2):1088-99.
12. Odhar HA, Ahjel SW, Albeer AA, Hashim AF, Rayshan AM, Humadi SS. Molecular docking and dynamics simulation of FDA approved drugs with the main protease from 2019 novel coronavirus. Bioinformation. 2020;16(3):236.
13. Dyall J, Coleman CM, Hart BJ, Venkataraman T, Holbrook MR, Kindrachuk J, Johnson RF, Olinger GG, Jahrling PB, Laidlaw M, Johansen LM. Repurposing of

clinically developed drugs for treatment of Middle East respiratory syndrome coronavirus infection. Antimicrobial agents and chemotherapy. 2014 Aug 1;58(8):4885-93.

14. Dong L, Hu S, Gao J. Discovering drugs to treat coronavirus disease 2019 (COVID-19). Drug discoveries & therapeutics. 2020 Feb 29;14(1):58-60.

15. Chan-Hui PY, inventor; Theraclone Sciences, Inc., assignee. Human Rhinovirus (HRV) Antibodies. United States patent application US 14/449,948. 2014 Nov 20.

16. Ray, Dr. Amit. "7 Limitations of Molecular Docking & Computer Aided Drug Design and Discovery." AMITRAY.COM. https://amitray.com/7-limitations-of-molecular-docking-computer-aided-drug-design-and-discovery/ Accessed 17-May-2020